The relationship between tension and slowly varying intracellular calcium concentration in intact frog skeletal muscle

D. L. Morgan *, D. R. Claflin † and F. J. Julian

*Department of Anesthesia Research Laboratories, Harvard Medical School, Brigham and Women's Hospital, Boston, MA 02115-6195, USA and *Department of Electrical and Computer Systems Engineering, Monash University, Clayton, Victoria 3168, Australia*

1. The relationship between intracellular calcium concentration, $[Ca^{2+}]_i$, and fixed-end tension was investigated in intact single muscle fibres from frogs. A slow decline of tension was produced by cyclopiazonic acid (CPA), a sarcoplasmic reticulum Ca^{2+} uptake pump inhibitor. The fluorescent dyes fura-2 and furaptra (mag-fura-2) were used to estimate $[Ca^{2+}]_i$.

2. Neither the steepness nor the position of the curve changed consistently over a wide range of tension decay times from a few seconds to over 100 s. For these near-steady-state curves, the 10–90% tension change occurred, on average, in 0·07 pCa units, corresponding to a Hill coefficient > 25, much steeper than previously reported. Possible artifacts could reduce that to 15.

3. Methoxyverapamil (D600) reduces the calcium released in response to an action potential. Contractions with D600 and CPA had a slow rise composed of many small steps, and a slow fall. Comparing rise and fall showed little or no hysteresis in the tension–$[Ca^{2+}]_i$ relationship.

4. A model involving co-operativity between the binding of Ca^{2+} and myosin to thin filaments is shown to produce a tension–pCa relationship that is substantially altered by the mean rate constant for detachment of myosin cross-bridges, which in turn is likely to be affected by sarcomere movements.

5. Such a model is shown to be capable of reproducing the small rise in $[Ca^{2+}]_i$ previously reported during the late phase of fixed-end relaxation of intact fibres.

In skeletal muscle, activation is normally controlled by the release of Ca^{2+} from the sarcoplasmic reticulum into the myoplasm, where it binds to the low-affinity Ca^{2+}-specific sites of troponin-C (TnC), causing poorly understood alterations in the thin filament that allow myosin heads to bind (or bind strongly) to the actin filaments and generate tension (Rüegg, 1988). The relationship between the intracellular calcium concentration ($[Ca^{2+}]_i$) and tension is an important factor in understanding this process. During either twitch or tetanic activation of an intact fibre, the $[Ca^{2+}]_i$ is seen to be continually and rapidly varying, when observed with a rapidly respding indicator (Konishi, Hollingworth, Harkins & Baylor, 1991) and, under these conditions, a plot of tension against $[Ca^{2+}]_i$ is not the steady-state relationship. This relationship has therefore been investigated almost exclusively by the use of skinned fibres, where the sarcolemma has either been removed or made permeable to most soluble species. While this enables maintenance of a steady $[Ca^{2+}]_i$, it is likely to change the myoplasmic composition significantly, as well as possibly altering significant structural relationships between the contractile proteins.

The steady-state tension–pCa relationship is typically characterized by two parameters: the $[Ca^{2+}]_i$ for 50% tension, or steady-state $[Ca^{2+}]_{50}$, and a measure of the steepness, usually N, the coefficient in a fitted Hill curve (Hill, 1913). This represents the number of maximally co-operative sites (each must be filled in turn) involved in a reaction. It was apparent even from very early work on skinned fibres (Julian, 1971) that the Hill coefficient for skinned muscle activation exceeds the number of low-affinity calcium binding sites per TnC molecule; two in skeletal muscle and one in cardiac. This implies that there must be co-operativity between TnC molecules, not just between binding sites on each molecule. There continues, however, to be a wide range of reported values, mainly near four but up to eight (Fig. 7.1 of Mulligan, 1989) in permeabilized skeletal muscle and two to three in cardiac muscle (reviewed in Bers, 1991, p. 27).

† To whom correspondence should be addressed.

While several models have been proposed to account for the high values, we know of no model that accounts for this variability. (For references to models, see Modelling in Methods.)

Sarcoplasmic Ca^{2+}-uptake pump inhibitors can be used to slow the relaxation of intact muscle fibres. If the decline in tension and $[Ca^{2+}]_i$ is made 'slow enough', a pseudo-steady state should exist, so that the tension–pCa curve could be plotted from a single relaxation. Hill coefficients with mean values of 6·0 (Yue, Marban & Weir, 1986; Dobrunz, Backx & Yue, 1995) were found in recent experiments using such inhibitors with cardiac muscle and the ratiometric dye fura-2. A Hill coefficient of 5·1 was found in similar experiments with single mouse fibres using indo-1 (Westerblad & Allen, 1993). We report here similar experiments on frog single skeletal muscle fibres, in which much higher values for the Hill coefficient were found.

Another observation that has been interpreted as evidence of Ca^{2+}–myosin co-operativity is the rise in $[Ca^{2+}]_i$ following the shoulder during relaxation in an isometric tetanus, seen by Cannell (1986) using aequorin, and by Julian, Claflin, Morgan & Stephenson (1992) and Caputo, Edman, Lou & Sun (1994), both using fluo-3. We know of no reports where ratios of fluorescence signals have been used to ensure that movement artifacts were eliminated. No quantitative model of this phenomenon has been reported. However, models that include calcium–myosin co-operativity seem likely candidates, and were therefore investigated.

It has been shown (Zahalak & Ma, 1990) that a 'tight coupling' model, in which release of Ca^{2+} cannot precede unbinding of myosin, can reproduce the related phenomenon of a rise in $[Ca^{2+}]$ in response to a release during relaxation of a twitch, but a 'loose coupling' model cannot. The model of Westerblad & Allen (1994) adapted here is in between the tight coupling and loose coupling models of Zahalak & Ma (1990), in that release of Ca^{2+} is possible without release of myosin, but binding of Ca^{2+} and myosin are not totally independent. Indeed, during most of relaxation the fraction of cross-bridges attached exceeds the fraction of TnC with Ca^{2+} bound.

METHODS

Single muscle fibres were dissected from the tibialis anterior muscles of the frog *Rana temporaria*. Frogs were killed by decapitation followed by double pithing, after being immersed in ice-cold water for no less than 10 min. Dissection and the experimental chamber were as previously described (Claflin, Morgan, Stephenson & Julian, 1994). For these experiments, the chamber was mounted on a Nikon Diaphot 300 inverted microscope fitted with a PTI (Photon Technology International, South Brunswick, NJ, USA) photometer system and a PTI Deltascan 4000 illumination system. All experiments were done at 3·0 °C. The standard Ringer solution contained (mM): 115 NaCl, 2·5 KCl, 1·8 $CaCl_2$, 2·15 Na_2HPO_4, 0·85 NaH_2PO_4; pH 7·2.

Cyclopiazonic acid (CPA) was introduced by incubating the fibre in Ringer solution containing 1 μM CPA (Sigma Chemical Co.) for at least 30 min. In a preliminary experiment, the resting fura-2 ratio was found to stabilize after 20 min.

For two experiments using fura-2, methoxyverapamil (D600) (Sigma Chemical Co.) was used to reduce the amount of calcium released due to each action potential (Berwe, Gottschalk & Lüttgau, 1987). Such fibres were paralysed by a single potassium contracture in 8 μM D600, and controlled warming was used to produce the desired state of partial paralysis (Claflin, Morgan & Julian, 1990). Stimulation at a slow rate, typically one pulse per 2 s, led to a tension rise that consisted of a series of small rapid rises with periods of slowly declining $[Ca^{2+}]_i$ and tension between them. The stimulus times were determined as the positive-going zero crossings of the differentiated tension records, and the ratio and tension for that step taken as the average over the three samples preceding each stimulus.

This and all other data analysis was performed using the program Igor (Wavemetrics, Lake Oswego, OR, USA), running on Macintosh computers.

Monitoring $[Ca^{2+}]_i$

For these experiments, only ratiometric dyes were used, specifically fura-2 and furaptra (also known as mag-fura-2; Molecular Probes). Ratiometric dyes allow correction of the signal for motion artifacts, i.e. changes in light signal caused by variations in the amount of dye contributing to the signal, either through translation or rotation of the fibre, or through movement of the fibre relative to the focal plane of the microscope. For these dyes, the sample is alternately illuminated with two excitation wavelengths, centred on 380 and 344 nm, set by diffraction grating monochromators (monochromator entrance and exit slit widths corresponding to 1·5–2 nm for photon counting and 10 nm for analog recording) and the fluorescence monitored in a 40 nm band centred at 510 nm, set by a filter (Omega Optical, Brattleboro, VT, USA). In view of the difficulty of obtaining exactly repeatable contractions in the presence of CPA, the alternating of the excitation wavelength was not done on a contraction-by-contraction basis, but by 'chopping' the incident illumination with the spinning toothed mirror of the illuminator. For fura-2, the photomultiplier was used in photon-counting mode, and the fluoresence calculated by the PTI software at the requested rate, usually ten measurements per second. For furaptra, in order to reduce noise in view of its low sensitivity to $[Ca^{2+}]$, the photomultiplier was used in analog mode, at higher light intensities than would have been possible in photon-counting mode. In this case an analog signal proportional to the light was recorded on a digital oscilloscope (Nicolet 4094, Madison, WI, USA) typically using a 10 ms sampling interval, and the fluorescence at the two wavelengths extracted by discarding the samples either side of a zero crossing and averaging the acquired samples from each illumination period. The effective signal bandwidth was thus the chopping frequency of about ten samples of each excitation wavelength per second. The relatively small background and auto-fluorescence signal, produced by illuminating the chamber and fibre before adding dye, was subtracted at each excitation wavelength, and the ratio R of the dye fluorescence at 344 nm to that at 380 nm was formed. The excellent cancellation of motion signals that resulted, and that allowed us to work at full filament overlap length, is shown in Fig. 1. Here, unrealistically large motion signals were introduced by manually moving the microscope stage to translate a fibre laterally out of the field of view, so that the light signals disappeared entirely, but the ratio signal merely became noisier due to the decreased light intensity, without any consistent change in value. The field of view was defined by an adjustable rectangular mask in the light path, and was set to be 1·16 mm long by 0·3 mm wide at the fibre. By comparison, the typical fibre length was 7 mm at a sarcomere length of 2·2 μm, as used throughout these experiments.

Dye was introduced by soaking the fibre in a solution containing 15 μM fura-2 for 60 min at 20 °C or in 10 μM furaptra for 30 min at 20 °C. Both dyes were present as the acetoxymethyl ester (AM) form, and the dispersing agent Pluronic F-127 (0·01% w/v; Molecular Probes) was used. Fura-2 has a greater sensitivity to Ca^{2+} than has furaptra, as well as being less affected by magnesium. However, the greater sensitivity means greater non-linearity between changes in ratio and changes in $[Ca^{2+}]_i$ as R approaches R_{max} (see below). For furaptra, the ratio is always very close to R_{min} compared with any reasonable estimate of R_{max}, so that linearity is assured. Similar results from both dyes provide assurance that distortion due to saturation was not significant for fura-2. Fura-2 is also unable to follow rapid transients as faithfully as furaptra (Konishi *et al.* 1991), though that was not a consideration in these experiments.

Dye parameters

The myoplasmic $[Ca^{2+}]$ was estimated from the ratio using the standard formula:

$$[Ca^{2+}] = K_D\beta(R - R_{min})/(R_{max} - R)$$

(Grynkiewicz, Poenie & Tsien, 1985). Although the calculation of Hill coefficients of tension–pCa curves are essentially independent of the dye parameters assumed, as is shown in Appendix I, estimates of the parameters were made. The minimum (R_{min}) and maximum (R_{max}) ratios were determined by exposing cells to the calcium ionophore 4-bromo-A23187 (Calbiochem, La Jolla, CA, USA), using methods based on those of Williams & Fay (1990). The R_{min} solution, used for fura-2, contained (mM): 115 NaCl, 2·5 KCl, 0·85 NaH_2PO_4, 2·15 Na_2HPO_4, 1 $MgCl_2$, 2 EGTA; and 10 μM 4-bromo-A23187; pH 7·2. The R_{max} solution was normal Ringer solution (1·8 mM Ca^{2+}) with 10 μM 4-bromo-A23187, and 10 μM CPA added to completely block sarcoplasmic reticulum uptake of Ca^{2+}, and 10 mM 2,3-butanedione monoxime (BDM; Aldrich, Milwaukee, WI, USA) to reduce tension generation, so reducing movement and metabolic changes. The light signals were monitored in these solutions until the value reached a plateau. This time was 1–2 h for fura-2 R_{min}, 10–15 min for fura-2 R_{max}, and 30–90 min for furaptra R_{max}. Each fibre was used for only one determination.

For furaptra, the ratio in the resting fibre was taken as R_{min}, for the following reasons. Furaptra is also sensitive to $[Mg^{2+}]$, and the resting $[Mg^{2+}]$ in a fibre is comparable to the K_D for Mg^{2+}, i.e. the concentration at which half of the dye has Mg^{2+} bound. Because of this, a given percentage change in $[Mg^{2+}]$ or given change in pMg will produce a much greater change in R than the same percentage change in $[Ca^{2+}]_i$, or same change in pCa. Consequently, the small variations in the resting ratio seen between fibres were considered more likely to reflect variations in resting $[Mg^{2+}]$ than resting $[Ca^{2+}]_i$. In these circumstances, the resting ratio in a given fibre is the best estimate of the ratio at zero $[Ca^{2+}]_i$ in that fibre.

The value of the third parameter of the calibration curve, $K_D\beta$, was taken as the product of β from the R_{max} and R_{min} experiments and K_D from the *in vitro* measurements (Table 1). As discussed in Appendix I, it does not affect the steepness of the estimated tension–pCa curve.

Characterizing tension–pCa curves

We found it preferable to characterize the steepness of the tension–pCa curve in terms of the difference in pCa between 90 and 10% maximal tension (ΔpCa). This is simply because, for very steep relationships, small changes in the steepness result in large changes in N, which tends to infinity as the $[Ca^{2+}]_i$ at 90% approaches that at 10% tension. Clearly, average values of N are not meaningful under these conditions. The dual vertical axes in Fig. 5 show the relationship between them, $\Delta pCa = (\log_{10}81)/N$, derived from the Hill equation (Hill, 1913).

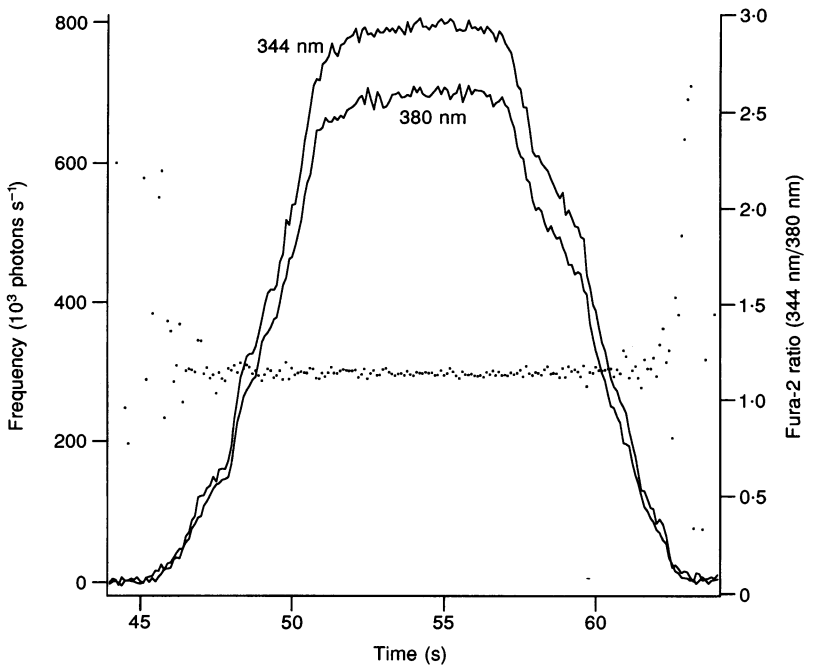

Figure 1. Removal of motion signal by taking the ratio of fluorescences

A fibre, loaded with fura-2, was moved laterally from one side of the mask, through the mask and out the other side. The two fluorescence signals (continuous lines, after subtraction of background and autofluorescence) changed proportionately, so that the ratio (points) became noisier as the fibre moved out of the mask, but did not change. Sampling rate, 10 per second; no other filtering.

Fitting of Hill curves in the usual way proved unsatisfactory, since the usual fitting procedure minimizes the root mean square (r.m.s.) value of the vertical distance between the points and the fitted line. In these tension–pCa plots, e.g. Fig. 3, the curve is near-vertical and the noise is mainly in the horizontal direction, i.e. in $[Ca^{2+}]_i$. For this reason curves were fitted to minimize the r.m.s. value of the horizontal distance between the data points and the fitted line. This is equivalent to exchanging the axes before fitting. The fitting process was modified further to fit only to data points with tension between 5 and 95% of maximum tension for that contraction. If this was not done, the fit was unduly influenced by the 'tail' of the relaxation, both because the tail contained many data points and also because any misfit in tension produced large differences in $[Ca^{2+}]_i$ between the points and the fitted line, strongly influencing the fit. Finally, some relaxations produced very steep or even multi-valued curves, where $[Ca^{2+}]_i$ rose slightly during some of the time that tension was falling, giving multiple values of tension for some particular values of $[Ca^{2+}]_i$. In order to fit these, the fitting routine was modified to pass ΔpCa rather than N as the parameter to the fitting equation. (N was derived from it for substitution into the Hill equation.) This meant that as the curve became steep, ΔpCa tended to zero, and if necessary became negative, rather than N becoming infinitely large. Consequently, for multivalued curves, the ΔpCa for optimum fit was negative. While the resulting fitted curve clearly did not fit the data below 5% tension (the fitted curve tending to zero tension for high rather than low $[Ca^{2+}]_i$), it did provide a much better fit to the central region of the curve than could be obtained by keeping $\Delta pCa > 0$. The overall effect of fitting multivalued curves on our conclusions was not significant, as most of the multivalued curves were for moderately rapidly falling contractions, which were excluded from our averaging (Fig. 5).

$[Ca^{2+}]_i$ rise during normal relaxation

Experiments were also undertaken to confirm the existence of the transient rise in $[Ca^{2+}]_i$ following the shoulder in the tension trace during fixed-end relaxation of a normal fibre, i.e. without CPA. For these experiments, fura-2 was used, with the excitation wavelength being alternated for alternate contractions. The signal for each wavelength was averaged over typically nine contractions, the background- and auto-fluorescences subtracted from the averaged signals, and then the ratio formed.

Modelling

The dynamic model was constructed using the program Stella (High Performance Systems, Hanover, NH, USA). This program allows construction of a model by drawing a block diagram consisting of stocks and flows. Both the basic structure and the constants were taken from Westerblad & Allen (1994), with the following changes. The maximum sarcoplasmic reticulum pump rate was set to 1 μM ms^{-1} (Cannell & Allen, 1984) rather than 4 μM ms^{-1} in Fig. 7 of Westerblad & Allen (1994) to represent frog rather than mouse muscle. The resting $[Ca^{2+}]_i$ was arbitrarily set at 0·1 μM, and the sarcoplasmic reticulum leak adjusted to match the pump rate at this free concentration. The possibility of Ca^{2+}–Ca^{2+} and myosin–myosin co-operativity was added, using equations of the same form as used for myosin–Ca^{2+} co-operativity by Westerblad & Allen (1994). An extra stock representing fura-2 (10 μM; 'on' rate constant (K_{on}) = 0·5 μM^{-1} ms^{-1}; 'off' rate constant (K_{off}) = 0·2 ms^{-1}) was added.

For steady-state calculations, two approaches were used. The first modified the Stella model to have a controlled myoplasmic $[Ca^{2+}]$, and calculated tension as steady state was approached. The second approach used Igor to calculate the steady state directly. By assuming a fraction of attached cross-bridges, simple equations derived from Westerblad & Allen (1994) allow calculation of the rate constants and concentrations of troponin with Ca^{2+} bound and hence free $[Ca^{2+}]_i$. The approach also handled multivalued curves without the need to try different initial conditions, as required in the Stella approach.

Statistical procedures

Statistical analysis used DataDesk (Data Description Inc., Ithaca NY, USA). Means are accompanied by their standard error. Significance statements are for $P = 0·05$ unless otherwise stated.

RESULTS

When 1 μM CPA was added to a fibre, the resting ratio rose slightly for about 20 min. At this time, stimulation produced a twitch with a slightly slowed relaxation. Only after repetitive stimulation did substantial slowing occur. However, cumulative changes, particularly increasing

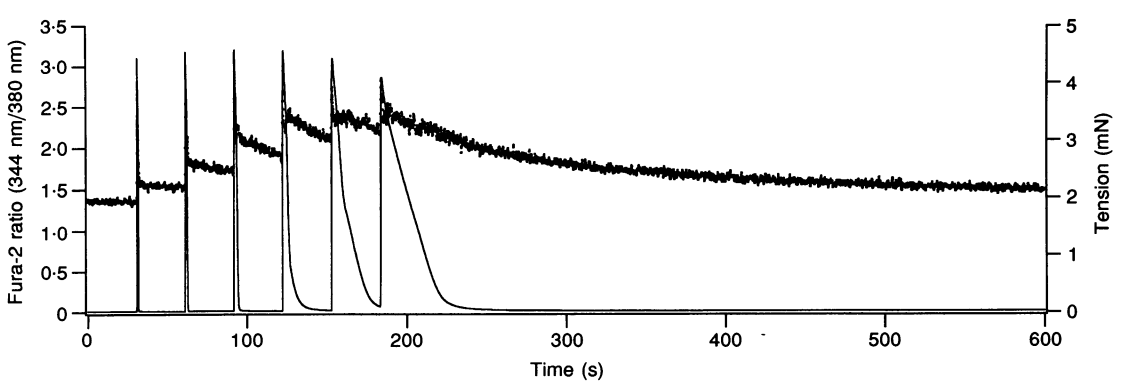

Figure 2. A typical recording from a fura-2-loaded fibre treated with 1 μM CPA, and subjected, every 30 s, to a pair of stimulus pulses separated by 50 ms

Each contraction relaxed more slowly than the previous, as shown by both tension (continuous line) and dye signal (points). When the fibre had failed to relax within 30 s, stimulation was stopped. This was the second series of tetani for this muscle, leading to the relatively high ratio at the beginning of the trace; a fibre that has been incubated in CPA but not stimulated has a fura-2 fluorescence ratio near 0·7.

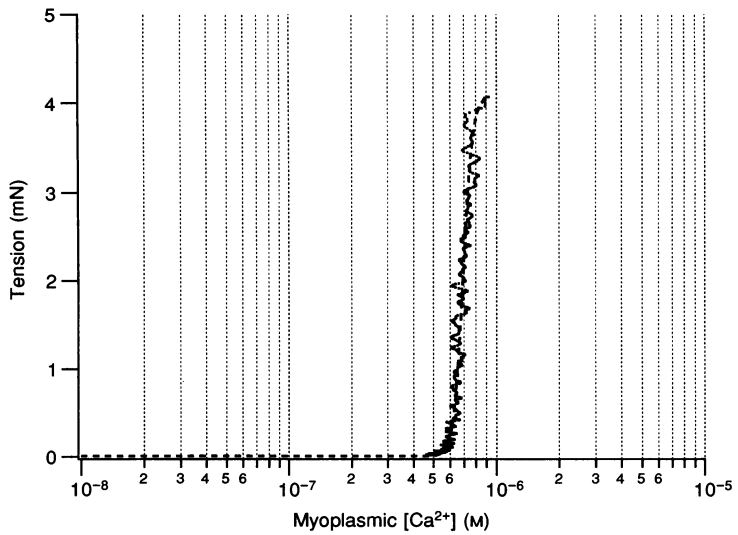

Figure 3. The tension–pCa curve during relaxation

This is the last contraction in Fig. 2, and the Hill curve fitted as described in Methods. Time between 10 and 90% tension = 32·6 s, $[Ca^{2+}]_{50}$ = 693 nM, N = 19·2, ΔpCa = 0·10.

relaxation times, were seen even with stimulation rates as low as one twitch every 10 min. This suggests that the sarcoplasmic reticulum Ca^{2+} uptake pump was significantly blocked, but that other relatively slow calcium binding sites in the myoplasm, presumably including parvalbumin, needed to be filled before relaxation was slowed significantly. We developed a protocol in which the fibre was stimulated with two stimuli separated by 50 ms, every 30 s for 10 min or until the tension had not relaxed fully in the 30 s interval, whichever occurred first. If slow relaxation did not occur within the first 10 min run, another was done after a 10 min rest. A typical record is shown in Fig. 2, where the stimulation was stopped after six contractions.

Fibres were routinely watched through the microscope during the slow relaxations using red (700 nm) light trans-illumination and a video camera, and were notable for the generally small amount of movement apparent, compared with a normal relaxation. For fibres using furaptra, these observations were confirmed by the small variations in the light signal during excitation at 344 nm, which is isosbestic for this dye.

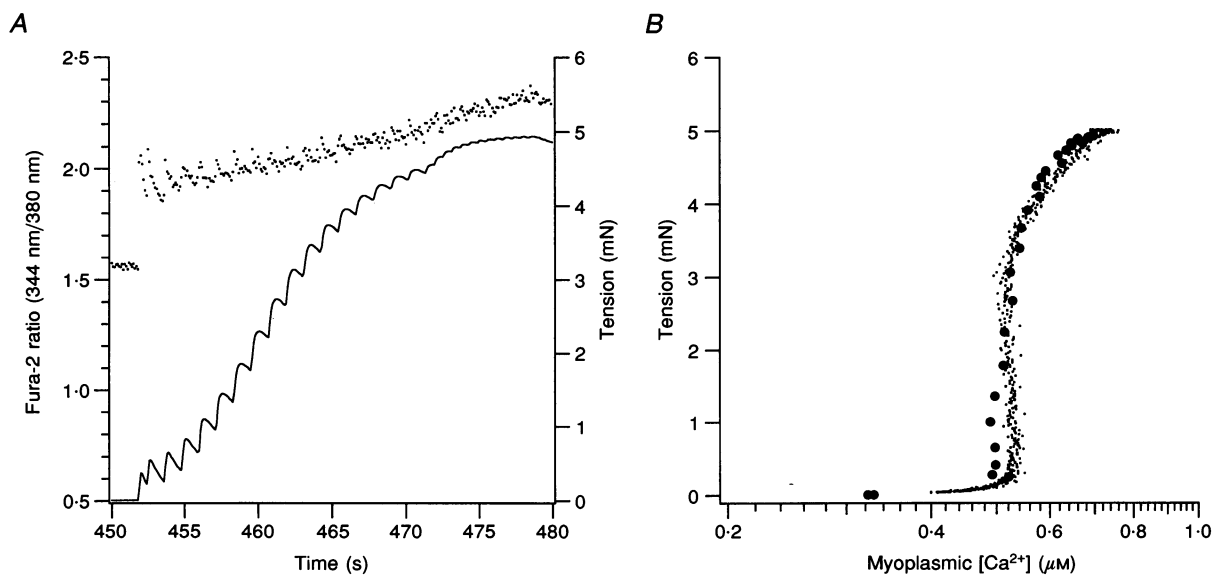

Figure 4. The rise and fall of tension in the presence of CPA and D600

A, tension (continuous line) and ratio (points) as a function of time. The interval between stimuli started as 2 s and then decreased to 1 s. *B*, the tension–pCa curve. Markers (●) are from the rise, being measured from *A* just before each stimulus. Points are the record of the adjacent fall in tension. Note the greatly expanded $[Ca^{2+}]_i$ scale. ΔpCa values were 0·08 for the rise and 0·07 for the fall.

Each relaxation of a record such as Fig. 2 was extracted, and tension plotted against the estimated $[Ca^{2+}]_i$ on a logarithmic scale, as in Fig. 3. All $[Ca^{2+}]_i$ estimates used the *in vivo* parameters in Table 1. A Hill curve was fitted (see Methods), and characterized by both the Hill coefficient, N, and ΔpCa, the logarithm of the ratio of $[Ca^{2+}]$ at 90% maximum tension to the $[Ca^{2+}]_i$ at 10% maximum tension, or the number of pCa units between these points on the fitted Hill curve. The tension–pCa curves measured in this way were extremely steep. Some relaxations, even very slow ones, gave multivalued curves, i.e. calcium rose slightly during some of the time that tension was falling, giving multiple values of tension for some particular values of $[Ca^{2+}]_i$. Possible causes of this counter-intuitive result are discussed in the Discussion.

If this is the steady-state relationship, then slowly *increasing* the $[Ca^{2+}]_i$ should produce a coincident tension–pCa curve. In order to check this we paralysed two fibres with D600, then warmed them slightly to produce near-complete paralysis. Under these conditions, D600 greatly reduces the amount of calcium released in response to stimulation, leading to very small twitches. When combined with CPA to slow the relaxation of the resulting twitches, contractions such as that shown in Fig. 4*A* were achieved. The tension rose in a near-staircase manner. Such low rates (one stimulus per 2 s), produced 50–80% of maximum tension, and in some tetani the rate was increased to one per second to more closely approach maximum tension. Such contractions were always very slow to relax.

Measuring tension and ratio just before the arrival of each stimulus pulse (see Methods), converting ratio to estimated $[Ca^{2+}]_i$ using the *in vivo* estimates of dye parameters in Table 1, and plotting on a logarithmic scale, gave points for the tension–pCa relationship during the rise of tension. A typical set of points is shown in Fig. 4*B*, along with the curve for the adjacent relaxation.

Any hysteresis was very small. The tension–pCa curve was very steep, with the average ΔpCa during rise being 0·178 (14 contractions) corresponding to an N value of 11. For the sixteen relaxations with relaxation times greater than 10 s in the same fibres, the mean ΔpCa was 0·132, corresponding to an N value of 14. The occurrence of steep curves for both rise and fall makes it unlikely that the steepness is due to the dynamics of the fall, i.e. that the tension is falling too rapidly for equilibrium to be reached. However, this point was investigated further by plotting the ΔpCa against the time taken for tension to decline from 90 to 10% of the maximum value reached in that contraction. This is shown for all experiments combined in Fig. 5. The logarithmic time scale is used to reduce crowding of the points.

For relaxation times greater that a few seconds, there is little consistent change in the ΔpCa, certainly no indication that the Hill coefficient would approach 2 or even 4 if the

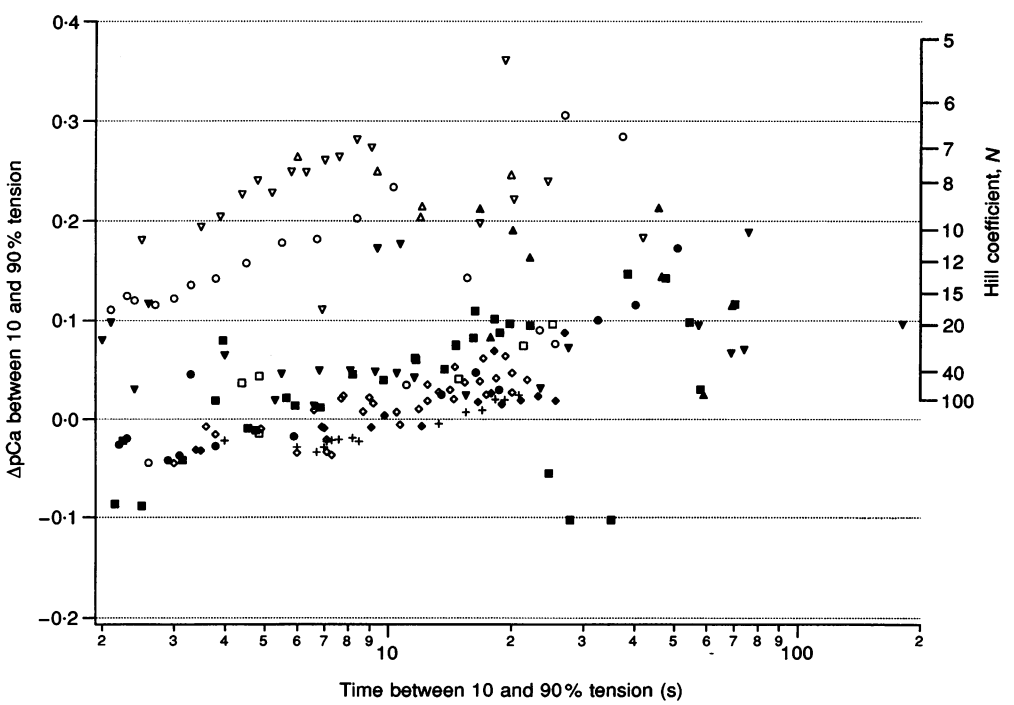

Figure 5. Collected parameters of the fitted Hill curves as a function of the rise or fall time

The right-hand axis is the Hill coefficient N on a non-linear scale, while the left-hand axis is ΔpCa, the number of pCa units between 10 and 90% of maximum tension along the fitted curve. Negative values indicate that the $[Ca^{2+}]_i$ at 90% was less than at 10% tension. Upward pointing triangular symbols are from slow rises in the presence of D600. Squares are from experiments using furaptra. Different symbols indicate different fibres.

relaxation was slowed further. Linear regression showed no significant correlation. If all 222 relaxations with times to fall from 90 to 10% greater than 1 s were included, the mean ΔpCa was 0·063 pCa units. For more rapid relaxations, the signal sampling rate was insufficient for a meaningful fit. The mean ΔpCa for relaxation times greater than 5 s (130 contractions) was 0·068 pCa units. For relaxation times greater than 10 s, the mean ΔpCa was 0·072 ($n = 84$). Normal relaxation time for a twitch at this temperature is in the 0·2–0·4 s range.

Although Fig. 5 suggests that ΔpCa is similar for rapid and slow relaxations, the small difference in ΔpCa between rapid and slow relaxations makes it difficult to judge how slow a relaxation needs to be for the binding to remain at steady state. A better idea of how slow is slow enough comes from plotting the $[Ca^{2+}]_i$ at 50% tension, or $[Ca^{2+}]_{50}$, which equals the steady-state $[Ca^{2+}]_{50}$ if the decay is slow enough to attain steady state. For normal fibres, the $[Ca^{2+}]_i$ has returned to near-baseline before the tension falls (Claflin *et al.* 1994) so both the $[Ca^{2+}]_{50}$ and ΔpCa would be near zero.

Figure 6 shows the way in which the $[Ca^{2+}]_{50}$ increased as the decay became slower for all the relaxations of one fibre, including the first contractions after the fibre was exposed to CPA. When further slowing does not raise the $[Ca^{2+}]_{50}$, then the decay must be slow enough that the tension–pCa relationship can be taken as equilibrium. For the fibre shown in Fig. 6, $[Ca^{2+}]_{50}$ increased steeply for relaxation times up to 3 s, much less steeply between 3 and 10 s, and very little thereafter. This was typical of other fibres. Combining these results with the statistics of Fig. 5 led us to adopt a relaxation time greater than 10 s as being near steady state, giving a best estimate for mean ΔpCa of 0·072 ± 0·009 (mean ± S.E.M.), corresponding to an N value most probably of 26·5, with a 5–95% probability range for mean ΔpCa corresponding to N values of between 22 and 33. If contractions were separated by dye, sixty-two contractions with fura-2 gave a mean ΔpCa of 0·075, corresponding to $N = 25·3$, and twenty-two contractions with furaptra gave a mean ΔpCa of 0·063, corresponding to $N = 30·5$. An ANOVA showed that neither dye nor relaxation time were significant determinants of ΔpCa, but that it did vary significantly between fibres.

Rise in $[Ca^{2+}]_i$ as tension falls in normal fibres

These experiments, previously done with fluo-3, were repeated using fura-2, enabling the experiments to be done at full overlap with motion artifacts being removed by taking the ratio. The previous observations were confirmed. In particular, the ratio fell during the linear phase of relaxation, and paused or rose during the rapid phase of relaxation, as shown for a twitch in Fig. 7*A*. The rise is larger after a tetanus, but it can be seen after a twitch if the twitch shows a clear shoulder during relaxation. It should be noted that this rise in $[Ca^{2+}]_i$ during a fall in tension corresponds to a multivalued dynamic tension–pCa curve.

Modelling

Models of activation to fit such steep curves incorporate one or more types of co-operativity in the activation process. We broadly grouped these into three types. In Ca^{2+}–Ca^{2+} co-operativity, the binding of one calcium ion to a TnC molecule enhances the binding of calcium ions to neighbouring TnC molecules in the same thin filament (Hill, 1983; Dobrunz *et al.* 1995). In myosin–myosin co-operativity, the binding of one myosin head to a thin

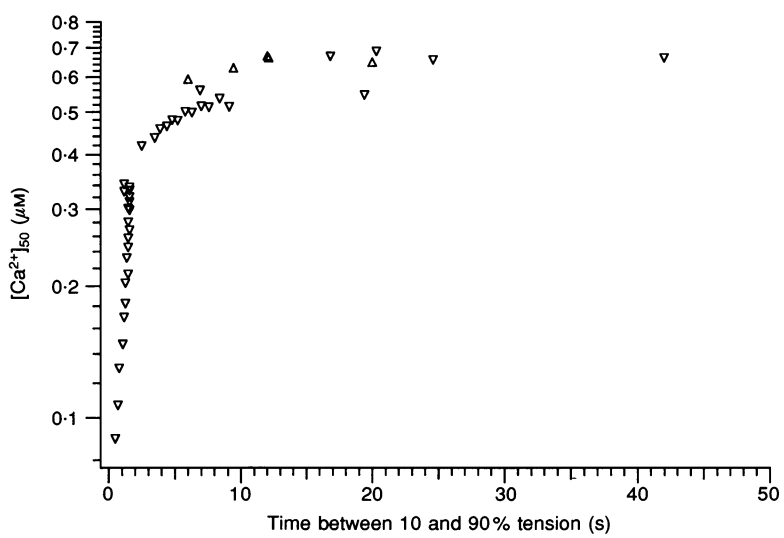

Figure 6. The variation of the $[Ca^{2+}]_i$ at 50% tension with the time of fall or rise for one experiment

Falls slow enough to approach the limiting value were assumed to be near equilibrium. Rapid relaxations had much smaller $[Ca^{2+}]_{50}$ values. Upward pointing triangles are rises. Downward pointing triangles are falls.

filament enhances the binding of more myosin heads (Goldman, Hibberd & Trentham, 1984; Metzger, 1995). In myosin–Ca^{2+} co-operativity, the binding of myosin enhances the binding of Ca^{2+} (Güth & Potter, 1987; Lehrer, 1994; Westerblad & Allen, 1994; Fuchs, 1995). Of course, two or all three of these mechanisms may be present in muscle (Shiner & Solaro, 1982; Ashley, Mulligan & Lea, 1991).

Cross-bridge detachment rate constants

Myosin–Ca^{2+} co-operativity can be explored in a mathematical model such as that of Westerblad & Allen (1994), where the detachment rate of Ca^{2+} from troponin is modified by the number of attached (tension-generating) myosin cross-bridges. The models described here were closely based on this. A feature of this model, not mentioned by the authors, is that the tension–pCa curve depends on the 'detachment rate for cross-bridges' (G in their Fig. 1, B in the text). In such a simple two-state model, G is actually the mean detachment rate constant, corresponding, in an A. F. Huxley model (Huxley, 1957), to a weighted average of $g(x)$ over the current cross-bridge distribution, $n(x,t)$. Formally:

$$\bar{g}(t) = \frac{\int g(x)\, n(x,t)\, \mathrm{d}x}{\int n(x,t)\, \mathrm{d}x},$$

where x is the displacement of the binding site on the actin filament from the position at which the cross-bridge would generate zero force if it was attached, $g(x)$ is the detachment rate constant for an attached cross-bridge as a function of x, t is time and $n(x,t)$ is the fraction of cross-bridges attached at displacement x and at time t. We suggest the symbol $\bar{g}(t)$ (the mean detachment rate constant for cross-bridges at a given time) to emphasize the averaging and the variation with time if the cross-bridge distribution is changing. According to Huxley's model, $\bar{g}(t)$ will be small in isometric sarcomeres, but larger in sarcomeres that are either lengthening or shortening, where more of the cross-bridges have a distortion that is associated with a high $g(x)$.

Within the range of cross-bridge distortions over which attachment can occur, Huxley (1957) chose $g(x) = g_1 x$. The magnitude of g_1 has been the subject of considerable conjecture. Huxley (1957) originally chose it to reproduce the second, exponential phase of relaxation, then found that this was determined mainly by internal movement, and suggested that g_1 should be more properly chosen to match the initial slow, linear phase of relaxation (Huxley & Simmons, 1972). However, this rate is very variable, and the cause of its variation is not clear. Huxley & Simmons (1972) showed that adding a segment length clamp to a well mounted single fibre substantially reduced the slow relaxation rate, suggesting that the rate was strongly dependent on even very small amounts of internal motion, and hence was determined primarily by unbinding of myosin. However, other experiments, including those of Hou, Johnson & Rall (1991) and our own unpublished observations, have shown that increasing the duration or the stimulation rate of a tetanus slows the relaxation, suggesting that the rate is determined primarily by the unbinding of calcium, and so influenced by the degree of

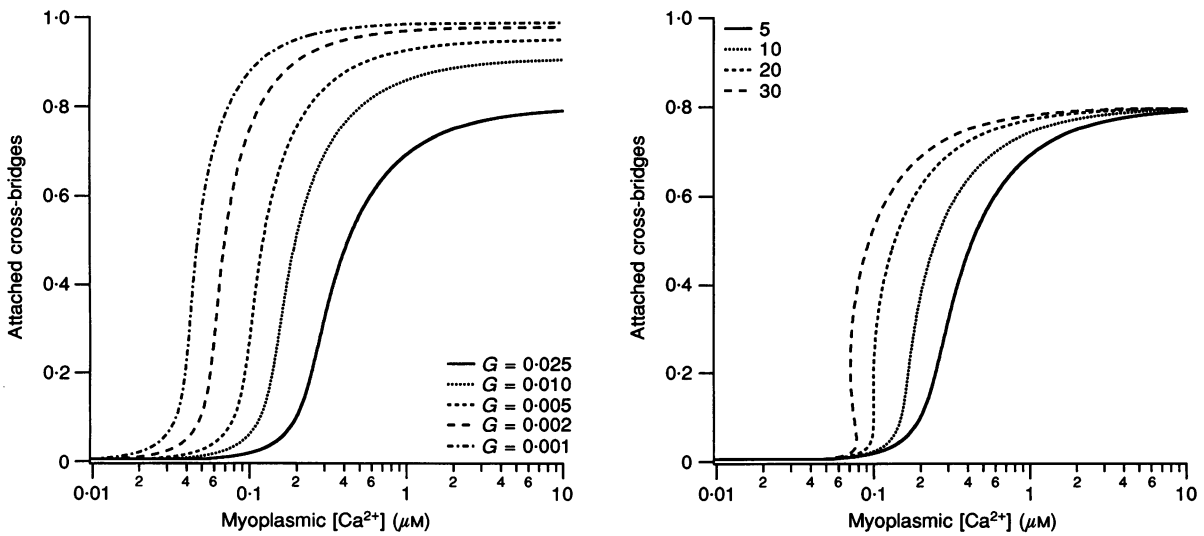

Figure 7. Modelling of tension–pCa curves

The left panel shows the effect of varying the mean cross-bridge detachment rate, $\bar{g}(t)$, corresponding to G in Westerblad & Allen (1994). Decreasing the cycling rate shifts the curve and makes it steeper. The right-hand panel shows the effect of varying the myosin–Ca^{2+} co-operativity beyond the value of 5 used by Westerblad & Allen (1994). Higher co-operativities gave steeper curves, and extreme values gave multivalued curves. However, this model could not produce the near-vertical plots seen experimentally for any values. In each case the continuous line is using the standard values, and only the nominated parameter was changed. In particular, all other co-operativities were set to zero.

saturation of parvalbumin with calcium. One way to reconcile these findings may be a model with high co-operativity between binding of Ca^{2+} and of myosin to thin filaments.

Description

We represented myosin–Ca^{2+} co-operativity by making the off rate constant for Ca^{2+} from TnC dependent on the proportion of attached bridges, as in Westerblad & Allen (1994; their eqn (4)). Ca^{2+}–Ca^{2+} co-operativity was similarly incorporated by making the attachment rate constant of Ca^{2+} to TnC dependent on the fraction of TnC with Ca^{2+} bound. Finally, myosin–myosin co-operativity was represented by making the off rate of cross-bridges depend on the fraction of cross-bridges attached.

Tension–pCa modelling

The first aim of the simulation was to explore how myosin–Ca^{2+} co-operativity interacted with $\bar{g}(t)$ to determine binding. We were interested in both the calcium bound to the regulatory sites of TnC (CaT) and tension, as functions of pCa. Figure 7 shows the effect of individually varying either the mean cross-bridge detachment rate constant or the myosin–Ca^{2+} co-operativity. The model curves were generated in the Igor steady-state simulation, and checked against the Stella transient model. The model used 100 data points, equally spaced over the tension range. It is clear that reducing $\bar{g}(t)$ moved the tension–pCa curve to lower $[Ca^{2+}]_i$ and made it steeper. Increasing the co-operativity had a similar effect, but could produce a multivalued curve. Increasing the co-operativity and reducing $\bar{g}(t)$ together produced a further shift to the left and increased steepness.

This result can perhaps be understood in the following way. A lower cross-bridge detachment rate constant means that a greater proportion of cross-bridges are attached for a given fraction of TnC with calcium bound, moving the curve to the left. More cross-bridges lead, by co-operativity, to a reduced rate constant for detachment of Ca^{2+}, reducing the free $[Ca^{2+}]_i$ required to maintain this occupancy. This effect is greater at high tensions, leading to increased steepness.

Attempts to produce model tension–pCa curves that closely matched the experimental ones were not highly successful. Figure 7 shows that increasing the degree of co-operativity beyond that suggested by Westerblad & Allen (1994) produced tension–pCa curves that were very steep or even had negative slope in the centre region, but were more rounded at high and low tensions than the experimental curves, and could not be well fitted by Hill curves. Alternative forms of co-operativity, Ca^{2+}–Ca^{2+} and myosin–myosin, also shifted the curve, but produced only small changes in the N value of the fitted curve. When combined with myosin–Ca^{2+} co-operativity, they also produced curves

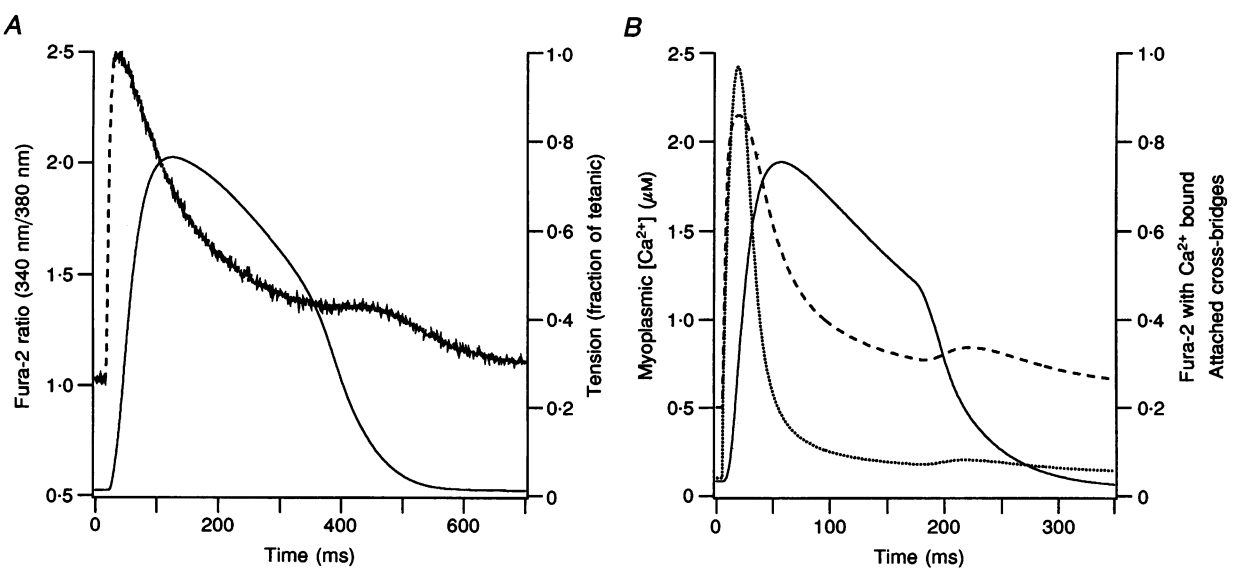

Figure 8. Comparison of experimental and simulated twitches

A, experimental results. Fura-2 ratio, interrupted line; tension, continuous line. Single fibre from *Rana temporaria* at 3 °C using fura-2. Average of 9 sweeps from each of four positions along one fibre. *B*, simulated twitch. Between 175 and 200 ms, the average cross-bridge detachment rate constant was increased from 0·015 to 0·045 ms^{-1}, to simulate an increase in internal motion. This produced the more rapid fall in tension (continuous line) and the rise in $[Ca^{2+}]_i$. The concentration of calcium bound to fura-2 (dashed line) differs from the myoplasmic $[Ca^{2+}]$ (dotted line) in that the main transient is attenuated by the dye dynamics more than the slower rise during relaxation. The fraction of cross-bridges attached (continuous line) is an indicator of tension. Only the amplitude of the sarcoplasmic reticulum permeability increase and the timing of the increase in $\bar{g}(t)$ were manipulated to optimize the match. Experimental tetani give larger rises, but the model does not simulate tetani well.

that became multivalued before reaching the experimental steepness as judged by the fitted curve.

Calcium rise during relaxation

The second aim of the model was to simulate the increase in $[Ca^{2+}]_i$ during relaxation. One way would be to have a truly multivalued tension–pCa curve, i.e. a true steady-state curve that had a region where tension increased as $[Ca^{2+}]_i$ decreased, giving multiple values of tension for one value of $[Ca^{2+}]_i$. This could certainly be generated by high co-operativity in both the steady-state model and the transient model, where it was manifest as hysteresis, i.e. a final tension value for a given $[Ca^{2+}]_i$ that depended on the initial value for tension. However, the experiments with D600 suggest that the tension–pCa curve for muscle has little or no hysteresis. The second way to show a $[Ca^{2+}]_i$ increase during relaxation was to make $\bar{g}(t)$ increase during relaxation in a model with myosin–Ca^{2+} co-operativity. An example of this is shown in Fig. 8*B*, and is compared with an experimental record in Fig. 8*A*.

Figure 8*B* was produced by the basic model described in Methods, with only the myosin–Ca^{2+} co-operativity described by Westerblad & Allen (1994), but with the $\bar{g}(t)$ increased linearly from 0·015 to 0·045 ms^{-1} between 175 and 200 ms, compared with the constant 0·025 ms^{-1} used by Westerblad & Allen (1994). This led to the shoulder in the tension curve, and the subsequent transient increase in $[Ca^{2+}]_i$. Clearly a more gradual rise in $\bar{g}(t)$ would produce a closer match to the experiment. Transient increases in $[Ca^{2+}]_i$ combined with single-valued steady-state tension–pCa curves were only seen in models that included myosin–Ca^{2+} co-operativity. Increasing $\bar{g}(t)$ can be seen as shifting the curve of CaT–pCa to the right. The prevailing myoplasmic $[Ca^{2+}]$ is then to the left of that appropriate to the existing tension and bound Ca^{2+}, leading to a rise in $[Ca^{2+}]_i$ as unbinding is increased and tension falls. In the absence of myosin–Ca^{2+} co-operativity, increasing $\bar{g}(t)$ does not shift the CaT–pCa curve. In this case the equilibrium of free and bound Ca^{2+} is not disturbed, and so no increase in unbinding occurs.

DISCUSSION

Possible artifacts

A major difficulty with the use of fluorescent dyes in contracting muscle is the elimination of motion artifacts. These can be reduced by stretching fibres to long length. They can be made less apparent by using a dye such as fluo-3, with little fluorescence at low $[Ca^{2+}]_i$, so that the signal is insensitive to movement while the fibre is relaxed. However, during the transient, changes in the amount of dye being observed will still produce a false signal. The use of ratios of light signals eliminates such problems extremely well. This is particularly important for both of the experiments reported here. In the CPA experiments, the contractions are prolonged, increasing the possibility of movement. In the observations of the rise of $[Ca^{2+}]_i$ during tension relaxation, the rise occurs at the point where movement of the fibre segment being observed is seen to suddenly increase, so motion artifacts must be carefully excluded. This has been done.

A second problem with fluorescent dyes is getting accurate estimates for their calibration parameters in the cell being studied. We found that R_{min} was similar *in vitro* and *in vivo*, but that R_{max} in our calibration fibres was variable and, on average, less than in buffer solution. The reasons for this are not yet clear, though the variable distribution of dye considered in Appendix II may be relevant. Changes in estimates of the dissociation constants affect the position of the tension–pCa curves, but not the shape (Appendix I). Therefore we did not attempt to determine the K_D as described by Williams & Fay (1990). Changes in R_{max} only affect the shape of the tension–pCa curve if the calibration curve is non-linear. For all the measurements using furaptra, the response could be considered linear (see Appendix I). In some fura-2 experiments, the ratio came unexpectedly close to our mean value for *in vivo* R_{max}, causing significant non-linearity in our assumed calibration relationship (Fig. 9), and hence relatively large ΔpCa values. It seems likely that the R_{max} for these fibres was greater than that measured in the fibres used for calibration. Consequently calibration errors are likely to have led to an over-estimate of ΔpCa (mean, 0·072), and correspondingly an underestimate for N (mean ΔpCa corresponds to $N = 26$). This view is supported by the steeper curves (mean ΔpCa corresponds to $N = 30$) for contractions with furaptra.

Another class of possible artifacts involve dye parameters that vary within a single fibre, either over the time course of a single slow relaxation, or over the course of an experiment. For example, Baker, Brandes & Weiner (1995) reported that the transient tension–pCa curve shifted with pH. Changes during a contraction are difficult to reconcile with the close agreement for rise and fall. In the case of pH, the fibre would be expected to become progressively acidotic during a slow rise of tension, as well as during a slow fall following a rapid rise of tension. Changes during the course of the experiment would be expected to lead to a progressive change in curve parameters over the course of the experiment, which was not seen. Also, contractions 30 s after the preceding contraction, i.e. during the same recording run, were not consistently different in tension–pCa steepness from the first contraction in a record, i.e. after a 10 min rest.

A final group of possible artifacts arises from the distribution of dye within the fibre. If the dye was concentrated around rather than within the myofibrils, it could be influenced by gradients near the sarcoplasmic reticulum produced by release from one point and uptake at another. However, the linear or near-linear response of these dyes means that they will register an average value of $[Ca^{2+}]$

in the region of the dye. Given that the length of a sarcomere is typically greater than the diameter of a myofibril, and the myofibril will contain no sources or sinks in the steady state, this is likely to be close to the average value within the myofibrils. It is also possible that some dye is in compartments other than the myoplasm, possibly with high $[Ca^{2+}]$. This raises many possibilities, considered in Appendix II, which concludes that the error in ΔpCa is unlikely to be more than 40%, whereas a Hill coefficient of 4, for example, corresponds to a ΔpCa 660% of that found here.

Approach to steady state

Treating the observed curve as the steady-state tension–pCa curve involves the assumption that these slow declines closely approximated steady state. In view of our arguments about the detachment rate of cross-bridges in the absence of motion being very low, it is possible that steady state is only attained in very slow relaxations. However, three pieces of evidence point to the idea that steady state was being reached. The first is simply that the mean ΔpCa did not change significantly when the threshold fall time for inclusion in the mean was raised above 5 s (Fig. 5). The second involves the $[Ca^{2+}]_i$ at 50% tension (Fig. 6). Although our absolute values should be treated with caution, the values from a single fibre can be meaningfully compared. If the contraction was not steady state, then a slower contraction should have given a higher $[Ca^{2+}]_{50}$, as was seen for short relaxation times. Beyond 10 s, however, $[Ca^{2+}]_{50}$ was almost independent of relaxation time. The third piece of evidence is the comparison of rising and falling tension (Fig. 4*B*). Although the match was not perfect, and the ΔpCa values for rising tension were on average somewhat higher than for falling tension in the same fibres, the coincidence was very good given the duration of the total contraction and associated fatigue of the muscle fibres. The values during the rise are of course actually taken during a series of slow falls between small rapid rises in response to stimuli, rather than during a smooth rise. However, the fact remains that the preceding histories at points of equal tension on the rise and fall are very different, but the observed $[Ca^{2+}]_i$ is very similar, indicating that the values are steady state.

Multivalued curves

The idea of a multivalued curve, i.e. a $[Ca^{2+}]_i$ that is higher at low tension than at high tension, is counter-intuitive. It seems that higher $[Ca^{2+}]_i$ must produce higher tension. There are, however, at least three ways in which this can arise experimentally. (1) The steady-state, sarcomere isometric curve really is multivalued. Our modelling shows that high degrees of co-operativity can give such a curve, as shown in Fig. 7. At higher tensions, the larger number of attached myosin cross-bridges increases the affinity of the thin filament for Ca^{2+}, so that the equilibrium free $[Ca^{2+}]$ is lower than at lower tensions, even though the fraction of troponin molecules with calcium ions bound is greater than at lower tensions. That is the change in affinity overwhelms the change in product concentration in influencing the equilibrium concentration of ligands. Such a curve should lead to hysteresis during rise and fall, which we did not see. (2) Under transient conditions the curve can be multivalued, even for a single-valued steady-state curve, as shown by the rise of $[Ca^{2+}]_i$ during fall in tension. This is likely to be the cause of the multivalued curves for shorter relaxation times. (3) If the amount of internal motion, and hence the mean rate of cross-bridge detachment, increased as the relaxation proceeded, then modelling suggests that the curve would appear steeper than for a constant detachment rate (moving from low to higher G values as tension falls in Fig. 7). That is, although more movement leads to a less steep curve, an increasing amount of movement during relaxation could lead to a steeper curve. This would also require a decreasing amount of movement during the rise of tension to match the curves for rising and falling tension (Fig. 4*B*).

Relation to other findings

The present tension–pCa results support and extend a recent trend towards steeper tension–pCa curves, particularly in intact preparations (see references in Introduction). Inclusion of myosin–Ca^{2+} co-operativity in the model, and the increased dependence of the tension–pCa curve on $\bar{g}(t)$ that this introduces (Fig. 7), provides one possible explanation for the variability of the reported N values, that N depends on the internal motion in the preparation. Hence the order of decreasing reported N values could be seen to be the order of increasing internal motion: intact frog fibres at low temperature, intact mouse single fibres, intact cardiac preparations, skinned skeletal fibres, and skinned cardiac preparations. Of course other factors may also be significant, including isoforms of troponin, species, and changes brought about by skinning.

The finding that any hysteresis in the tension–pCa relationship is small is in accord with previous work on skinned fibres (e.g. Brandt, Gluck, Mini & Cerri, 1985).

Significance

Such very steep tension–pCa curves as found here indicate a very high degree of co-operativity in the activation of muscle. In terms of function, a steep curve minimizes the amount of calcium that must be released from the sarcoplasmic reticulum to activate a muscle fibre, and returned to it at significant energetic cost, to bring about relaxation. Partial activation, such as a twitch, is then presumably attained, not so much by limiting the peak myoplasmic $[Ca^{2+}]$, but by returning it to low values before equilibrium is reached. A multivalued or hysteretic curve would be functionally undesirable, as it would require the calcium to be reduced further before the muscle could be relaxed, reducing the speed of relaxation that is important for locomotion and other tasks.

Table 1. Dye parameters measured under various conditions show considerable variability

Conditions	Fura-2			Furaptra		
	R_{min}	R_{max}	$K_D\beta$ (μM)	R_{min}	R_{max}	$K_D\beta$ (μM)
In vitro, no Mg^{2+}	0·61	15·8	1·76	0·349	18·4	730
In vitro, 1 mM Mg^{2+}	0·60	15·9	1·65	0·525	16·5	695
In vivo (mean of 4)	0·54 ± 0·01	5·31 ± 0·74	—	—	3·0 ± 1·2	—

For the 8 fibres used to calibrate fura-2 *in vivo*, the mean R at rest was 0·725 ± 0·086.

In terms of mechanism, such a steep curve without hysteresis can probably only be achieved by a combination of co-operative mechanisms. None of the simple co-operativity representations used in our modelling produced tension–pCa curves that matched the shape of the experimental curves very well. It remains to be seen whether more complex models of the mechanisms of co-operativity can simulate these observed curves (Lehrer, 1994; Dobrunz *et al.* 1995). The third mechanism for multi-valued curves suggested above may also contribute to the steepness.

Modelling of normal relaxation, and its accompanying transient increase in $[Ca^{2+}]_i$, strongly support the idea that there is co-operativity between calcium and myosin binding to thin filaments, whether or not other forms are also present.

Other evidence for and against myosin–Ca^{2+} co-operativity

The published body of evidence about co-operativity is too large to be fully reviewed here, but some comments are in order. Binding studies were reviewed by Ashley *et al.* (1991) and Gillis (1985), who both concluded that the evidence for myosin–calcium co-operativity was contradictory. Fuchs (1995) concluded that co-operativity was present in cardiac muscle but not in skeletal muscle, not even in slow skeletal muscle which has the same TnC isoform as cardiac muscle. Brandt, Diamond & Schachat (1984) found that removal of even 10% of the TnC reduced the steepness of the tension–pCa curve, indicating that troponin is involved in some part of the co-operativity. However, if the binding of TnC to actin filaments is itself co-operative, then the small fraction removed may not have been uniformly distributed among thin filaments, leading to increased internal motion. Popp & Maéda (1993) found that X-ray diffraction measures of activation were very steep, with a Hill coefficient apparently greater than 8, and possibly significantly greater. Güth & Potter (1987) found that myosin binding increased the apparent Ca^{2+} affinity for troponin tenfold as measured by dansylaziridine fluorescence in skinned fibres, though the Hill coefficient was less than 4. Again, variability in the amount of internal motion may account for some of the contradictory results.

Conclusions

We conclude that the apparent tension–pCa curve seen during slow relaxation of intact frog single fibres, induced by CPA, is very steep, with 90–10% relaxation typically taking place in 0·07 pCa units, corresponding to a Hill coefficient over 25. The presence of some dye in places other than the myoplasm could change these figures to 0·12 pCa units and approximately 15, respectively (Appendix II). This means that there must be extensive co-operativity involved in the activation of muscle. Modelling of the rise of $[Ca^{2+}]_i$ during normal relaxation leads to the conclusion that at least part of this co-operativity must be between calcium and myosin binding. The tight coupling model of Zahalak & Ma (1990) is one way, but not the only way, to introduce such co-operativity. The dependence of the tension–pCa curve on internal motion that this co-operativity introduces is suggested as an important cause of the range of tension–pCa parameters reported in the literature.

APPENDIX I

The effect of dye parameters on estimated tension–pCa steepness

The parameters of fluorescent dyes in intact fibres are subject to considerable uncertainties. To illustrate the uncertainty, Table 1 shows the values found for our equipment under various conditions. For the *in vitro* calibrations, six standard calcium buffers (Molecular Probes) were used in quartz microtubes mounted on the microscope stage, and the parameters found from the best fit of the relationship. In the intact fibres, only R_{min} and R_{max} were found for fura-2 and R_{max} for furaptra, as described in Methods.

It should be noted that these parameters are only appropriate for the light path as tested, as they depend on the lamp intensity at different excitation wavelengths, as well as the efficiency of the monochromators, filters, lenses and dichroic mirrors. Fortunately, this uncertainty in the parameters, provided they remain constant for a given fibre,

does not affect our conclusions regarding co-operativity, for the following reason.

Consider the conversion equation:

$$[Ca^{2+}] = K_D\beta\frac{R - R_{min}}{R_{max} - R}$$

$$= K_D\beta\frac{R - R_{min}}{(R_{max} - R_{min}) - (R - R_{min})}$$

(Grynkiewicz *et al.* 1985).

If the observed ratio change from zero $[Ca^{2+}]_i$, $R - R_{min}$, is much less than the $R_{max} - R_{min}$ of the dye, then the relationship between ratio changes and $[Ca^{2+}]_i$ is almost a straight line, as the denominator is essentially independent of R. This will be an accurate approximation for furaptra, and fair to good for fura-2, depending on the assumed R_{max}. (Note that the relationship between ratio and pCa is therefore far from linear over this region, the ratio being asymptotic to R_{min} as pCa tends to minus infinity (Fig. 9).) If the relationship between R and $[Ca^{2+}]_i$ is linear, then changing its slope will multiply the range of $[Ca^{2+}]_i$ during relaxation by the same factor as the $[Ca^{2+}]_i$ at mid-tension. When plotted as a tension–pCa curve (or with $[Ca^{2+}]_i$ on a logarithmic scale) the shape, and hence the Hill coefficient would be unchanged, as multiplication by a constant is seen as a shift on a logarithmic scale.

This conclusion was checked by analysing a given record with various assumed coefficients, and shown to be correct. The worst case is for fura-2, where using $R_{max} = 5{\cdot}31$ makes the calibration curve, shown in Fig. 9, significantly non-linear over the range of ratios seen in a tetanus, up to 3·5 at the peak of the transient, and up to 2·5 during the slow decline. This means that the change in ratio during relaxation is converted to a change in $[Ca^{2+}]_i$ using a steeper slope than is the $[Ca^{2+}]_i$ at 50% tension. If, however, the *in vitro* value was more nearly correct, then the calibration curve would be linear in this range. In a typical example, changing R_{max} from 5·3 (*in vivo*) to 15·9 (*in vitro*) decreased the ΔpCa from 0·094 to 0·062, and increased the Hill coefficient from 20·2 to 30·9.

For furaptra, the effects of the assumed dye parameters on the Hill coefficient were quite negligible for all reasonable values, though of course the steady-state $[Ca^{2+}]_i$ at 50% tension is affected by all the parameters.

APPENDIX II

The possible effects of some AM-loaded dye in other states than free in the myoplasm

Late in this investigation it came to our notice that some of the fluorescence of AM-loaded fura-2 is not removed by saponin, suggesting that some fura-2 is not free in the myoplasm (Endo & Iino, 1980). There are a number of possibilities as to where it might be, and a full investigation is beyond the scope of this paper. However, if the saponin-resistant dye was not influenced by myoplasmic $[Ca^{2+}]$ then it could provide a possible mechanism for an artifactually steep tension–pCa curve. In this case the observed fluorescence ratio changes would be smaller than expected for a given change in myoplasmic $[Ca^{2+}]$. This was investigated in some later experiments.

The first finding was that 20–50% of AM-loaded dye, as measured at the isosbestic point, was not removed by saponin (50 μg ml^{-1} for 30 min), with large variation between fibres. This is much more than the relative volume of the likely organelles, particularly sarcoplasmic reticulum and mitochondria. However, the greater ratio of surface area, which determines the amount of dye entering, to volume, which determines the resulting concentration, for organelles as compared with cells could theoretically cause accumulation of dye in organelles. This would be countered

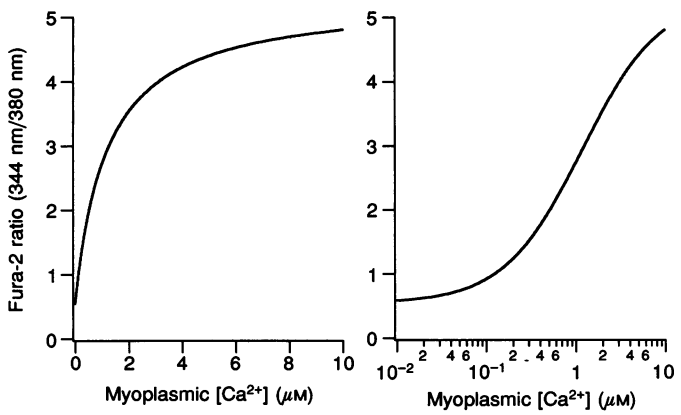

Figure 9. The calculated relationship between ratio and $[Ca^{2+}]_i$ for the *in vivo* parameters for fura-2 for linear and logarithmic $[Ca^{2+}]_i$ axes

This gives the greatest non-linearity at high $[Ca^{2+}]$ encountered in these experiments. Note that the relationship between $[Ca^{2+}]_i$ and R is near linear at low concentrations.

by the lower concentration gradient of the AM form across the mitochondrial membrane than across the cell membrane, particularly if the rate of entry of dye was limited by membrane permeability rather than enzyme activity. Virtually all of the saponin-resistant dye was removed by Triton X-100 (Sigma). Examination of the fluorescence of the dye remaining after saponin treatment in the presence of 2 mM EGTA and no added Ca^{2+}, revealed a 344 nm to 380 nm ratio near unity, i.e. more than expected in the absence of Ca^{2+} (0·54), and more than in a resting fibre (0·72), but far from the value expected in the sarcoplasmic reticulum with saturating [Ca^{2+}] (Table 1). Possibilities for this include the saponin and EGTA having only partly depleted a dye-containing compartment of Ca^{2+}, most of the dye being surrounded by low [Ca^{2+}], but a small fraction being in a high [Ca^{2+}] compartment, or the fluorescence arising from a different form of the dye, perhaps partially de-esterified or bound to some part of the cell.

In terms of their effect on our results, these possibilities can be grouped into three classes. (1) The saponin-resistant dye was still in the myoplasm and responding to the $[Ca^{2+}]_i$, perhaps resisting saponin treatment by being bound to some structure. In this case the normal analysis is appropriate. (2) The dye, possibly in the AM form, produces a constant fluorescence during contractions and after saponin treatment. In these cases, the appropriate treatment of data is to use the post-saponin-fluorescence as the background and autofluorescence (PSB&A) to be subtracted from the fluorescences during the contractions, before forming the fluorescence ratio.

To investigate this, three fibres underwent the normal experimental protocol, followed by saponin treatment, and the results are shown in Fig. 10. If only relaxation times greater than 10 s are considered, then the mean ΔpCa for the thirty-three contractions from these fibres with normal analysis was 0·028 ($N = 69$), and for PSB&A analysis, ΔpCa = 0·049 ($N = 39$). If all contractions with decay times greater than 5 s are considered, then the average ΔpCa for normal analysis is 0·012, corresponding to $N = 160$ (55 contractions). Using the PSB&A analysis, ΔpCa rises to 0·017, corresponding to $N = 113$. Clearly, changing to PSB&A analysis does make the curves appear less steep, but not sufficiently to affect our conclusions that a high degree of co-operativity must be present. If the average ΔpCa

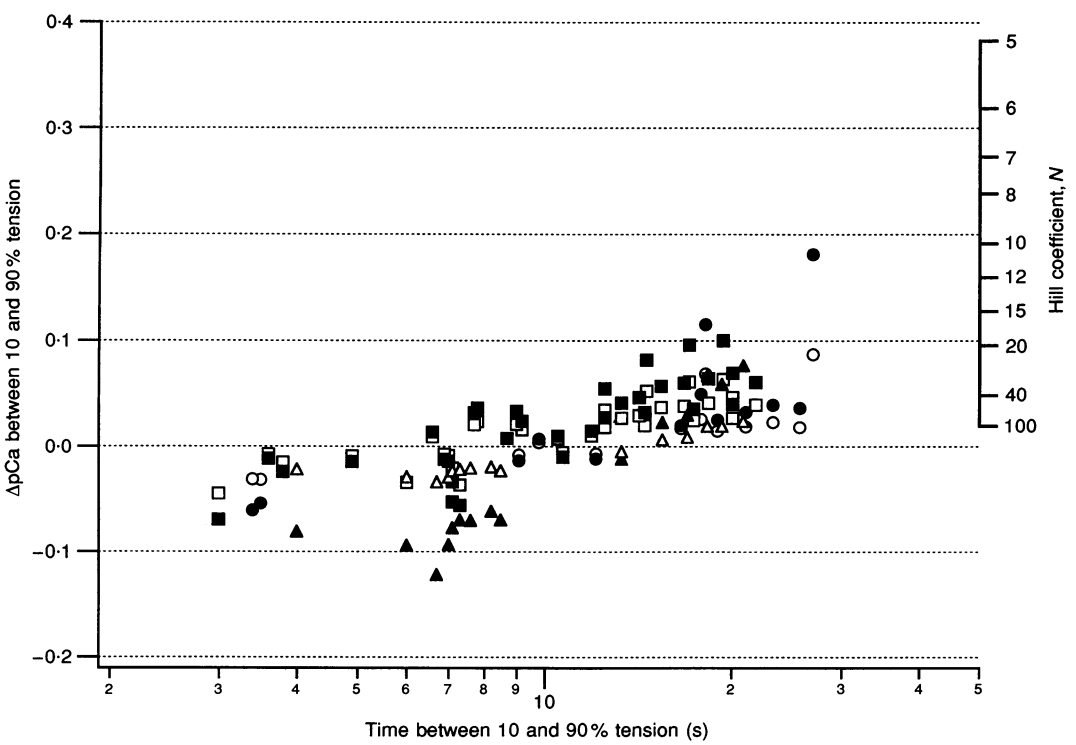

Figure 10. Hill curve parameters with normal and post-saponin autofluorescence adjustment

The axes are the same as for Fig. 5. The data points are from the 3 fibres for which saponin was used, analysed in two ways. Open symbols (normal) result from the normal analysis as described in Methods, and used for Fig. 5. Filled symbols are the same contractions as the open symbols, analysed using post-saponin background and autofluorescence (PSB&A), that is assuming that all the fluorescence remaining after treating the fibres with saponin and EGTA should be treated as background and autofluorescence. This treatment does increase the magnitude of the ΔpCa, but average values are still small. Circles, squares and triangles show results from different fibres.

averaged over all contractions with relaxation times greater than 10 s from all fibres is corrected in the same ratio, then the best estimate for N becomes 15.

(3) The third class of possible locations for the saponin-resistant dye is in a compartment where the $[Ca^{2+}]$ changes, making the above method unsuitable. The effect of this would depend on the time course of the changes of the $[Ca^{2+}]$ in that compartment. Most possible time courses are ruled out by the consistency of results over the course of an experiment, and the close correspondence of the relationships during rise and fall of tension (Figs 5 and 6). An exception is some compartment with a $[Ca^{2+}]$ that was low during loading, became raised by the first prolonged contracture, remained that way during the subsequent contractures, including the slow rises of tension and the rests between runs, but fell during the treatment with saponin. The mitochondria have been shown to meet some of these criteria. Substantial loading of mitochondria with fura-2 has been reported in hepatocytes under certain loading conditions (Jiang & Acosta, 1995). Mitochondria do take up Ca^{2+}, though reportedly more slowly than would be significant here. (Leisey, Grotyohann, Scott & Scaduto (1993) reported a half-time of 2 min at 20 °C for rat heart, and frog at low temperature would be expected to be much slower.) The release rate *in vitro* has been reported as being up to 1000 times slower than uptake, though with considerable uncertainty concerning the *in vivo* equivalence (Gunter, Gunter, Sheu & Gavin, 1994). An estimate of the effect of this scenario was made as follows. Our average value for ΔpCa was 0·07, corresponding on our calibration curve to a fluorescence ratio change of 0·18, occurring typically at a ratio of 2·25. If this is assumed to result from the worst case that we ever saw, i.e. two equal quantities of dye, one exposed to saturating $[Ca^{2+}]$ ($R = 5$), then the other half of the dye can be shown to have changed its ratio from 1·43 to 1·26. Converting these to $[Ca^{2+}]$ from the calibration curve gives a ΔpCa for the myoplasmic compartment alone of 0·110 or $N = 17$. That is the proposal results in a smaller correction than the use of post-saponin background and autofluorescence. Modelling of this showed that it comes about because a high assumed value for R for the saponin-resistant dye leads to a small R value for the myoplasmic dye, making the dye less saturated so that a given change in myoplasmic R indicates a smaller change in $[Ca^{2+}]$. Varying the assumed mitochondrial $[Ca^{2+}]$ and the distribution of dye, showed that the effect is similar for other reasonable values.

Ashley, C. C., Mulligan, I. P. & Lea, T. J. (1991). Ca^{2+} and activation mechanisms in skeletal muscle. *Quarterly Reviews of Biophysics* **24**, 1–73.

Baker, A. J., Brandes, R. & Weiner, M. W. (1995). Effects of intracellular acidosis on Ca^{2+} activation, contraction, and relaxation of frog skeletal muscle. *American Journal of Physiology* **268**, C55–63.

Bers, D. M. (1991). *Excitation–Contraction Coupling and Cardiac Contractile Force*. Kluwer Academic Publishers, Dordrecht, The Netherlands.

Berwe, D., Gottschalk, G. & Lüttgau, H. C. (1987). Effects of the calcium antagonist gallopamil (D600) upon excitation–contraction coupling in toe muscle fibres of the frog. *Journal of Physiology* **385**, 693–707.

Brandt, P. W., Diamond, M. S. & Schachat, F. H. (1984). The thin filament of vertebrate skeletal muscle co-operatively activates as a unit. *Journal of Molecular Biology* **180**, 379–384.

Brandt, P. W., Gluck, B., Mini, M. & Cerri, C. (1985). Hysteresis of the mammalian pCa/tension relation is small and muscle specific. *Journal of Muscle Research and Cell Motility* **6**, 197–205.

Cannell, M. B. (1986). Effect of tetanus duration on the free calcium during the relaxation of frog skeletal muscle fibres. *Journal of Physiology* **376**, 203–218.

Cannell, M. B. & Allen, D. G. (1984). Model of calcium movements during activation in the sarcomere of frog skeletal muscle. *Biophysical Journal* **45**, 913–925.

Caputo, C., Edman, K. A. P., Lou, F. & Sun, Y.-B. (1994). Variation in myoplasmic Ca^{2+} concentration during contraction and relaxation studied by the indicator fluo-3 in frog muscle fibres. *Journal of Physiology* **478**, 137–148.

Claflin, D. R., Morgan, D. L. & Julian, F. J. (1990). Earliest mechanical evidence of cross-bridge activity after stimulation of single skeletal muscle fibers. *Biophysical Journal* **57**, 425–432.

Claflin, D. R., Morgan, D. L., Stephenson, D. G. & Julian, F. J. (1994). The intracellular Ca^{2+} transient and tension in frog skeletal muscle fibres measured with high temporal resolution. *Journal of Physiology* **475**, 319–325.

Dobrunz, L. E., Backx, P. H. & Yue, D. T. (1995). Steady state $[Ca^{2+}]_i$–force relationship in intact twitching cardiac muscle: direct evidence for modulation by isoproterenol and EMD 53998. *Biophysical Journal* **69**, 198–201.

Endo, M. & Iino, M. (1980). Specific perforation of muscle cell membranes with preserved SR functions by saponin treatment. *Journal of Muscle Research and Cell Motility* **1**, 89–100.

Fuchs, F. (1995). Mechanical modulation of the Ca^{2+} regulatory protein complex in cardiac muscle. *News in Physiological Sciences* **10**, 6–12.

Gillis, J. M. (1985). Relaxation of vertebrate skeletal muscle. A synthesis of the biochemical and physiological approaches. *Biochimica et Biophysica Acta* **811**, 97–145.

Goldman, Y. E., Hibberd, M. G. & Trentham, D. R. (1984). Relaxation of rabbit psoas muscle fibres from rigor by photochemical generation of adenosine-5′-triphosphate. *Journal of Physiology* **354**, 577–604.

Grynkiewicz, G., Poenie, M. & Tsien, R. Y. (1985). A new generation of Ca^{2+} indicators with greatly improved fluorescence properties. *Journal of Biological Chemistry* **260**, 3440–3450.

Gunter, T. E., Gunter, K. K., Sheu, S.-S. & Gavin, C. (1994). Mitochondrial calcium transport: physiological and pathological relevance. *American Journal of Physiology* **267**, C313–339.

Güth, K. & Potter, J. D. (1987). Effect of rigor and cycling crossbridges on the structure of troponin C and the Ca^{2+}affinity of the Ca^{2+}-specific regulatory sites in skinned rabbit psoas fibers. *Journal of Biological Chemistry* **262**, 13627–13636.

Hill, A. V. (1913). The combinations of haemoglobin with oxygen and with carbon monoxide. I. *Journal of Biochemistry* **7**, 471–480.

Hill, T. L. (1983). Two elementary models for the regulation of skeletal muscle contraction by calcium. *Biophysical Journal* **44**, 383–396.

HOU, T.-T., JOHNSON, D. J. & RALL, J. A. (1991). Parvalbumin content and Ca^{2+} and Mg^{2+} dissociation rates correlated with changes in relaxation rate of frog muscle fibres. *Journal of Physiology* **441**, 285–304.

HUXLEY, A. F. (1957). Muscle structure and theories of contraction. *Progress in Biophysics and Biophysical Chemistry* **7**, 255–318.

HUXLEY, A. F. & SIMMONS, R. M. (1972). Mechanical transients and the origin of muscular force. *Cold Spring Harbor Symposia on Quantitative Biology* **37**, 669–680.

JIANG, T. & ACOSTA, D. JR (1995). Mitochondrial Ca^{2+} overload in primary cultures of rat renal cortical epithelial cells by cytotoxic concentrations of cyclosporine: a digitized fluorescence imaging study. *Toxicology* **95**, 155–166.

JULIAN, F. J. (1971). The effect of calcium on the force–velocity relation of briefly glycerinated frog muscle fibres. *Journal of Physiology* **218**, 117–145.

JULIAN, F. J., CLAFLIN, D. R., MORGAN, D. L. & STEPHENSON, D. G. (1992). Evidence for positive feedback between tension relaxation and Ca^{2+} release from regulatory sites in intact frog skeletal muscle fibers. *Biophysical Journal* **61**, A294.

KONISHI, M., HOLLINGWORTH, S., HARKINS, A. B. & BAYLOR, S. M. (1991). Myoplasmic calcium transients in intact frog skeletal muscle fibres monitored with the fluorescent indicator furaptra. *Journal of General Physiology* **97**, 271–301.

LEHRER, S. S. (1994). The regulatory switch of the muscle thin filament: Ca^{2+} or myosin heads. *Journal of Muscle Research and Cell Motility* **15**, 232–236.

LEISEY, J. R., GROTYOHANN, L. W., SCOTT, D. A. & SCADUTO, R. C. JR (1993). Regulation of cardiac mitochondrial calcium by average extramitochondrial calcium. *American Journal of Physiology* **265**, H1203–1208.

METZGER, J. M. (1995). Myosin binding-induced cooperative activation of the thin filament in cardiac myocytes and skeletal muscle fibers. *Biophysical Journal* **68**, 1430–1442.

MULLIGAN, I. P. (1989). Mechanical studies on skinned muscle fibres using caged ATP and caged calcium. PhD Thesis, University of Oxford.

POPP, D. & MAÉDA, Y. (1993). Calcium ions and the structure of muscle actin filament. An X-ray diffraction study. *Journal of Molecular Biology* **229**, 279–285.

RÜEGG, J. C. (1988). *Calcium in Muscle Activation.* Springer-Verlag, Heidelberg.

SHINER, J. S. & SOLARO, R. J. (1982). Activation of thin-filament-regulated muscle by calcium ion: Considerations based on nearest neighbor lattice statistics. *Proceedings of the National Academy of Sciences of the USA* **79**, 4637–4641.

WESTERBLAD, H. & ALLEN, D. G. (1993). The influence of intracellular pH on contraction, relaxation and $[Ca^{2+}]_i$ in intact single fibres from mouse muscle. *Journal of Physiology* **466**, 611–628.

WESTERBLAD, H. & ALLEN, D. G. (1994). The role of sarcoplasmic reticulum in relaxation of mouse muscle; effects of 2,5-di(*tert*-butyl)-1,4-benzohydroquinone. *Journal of Physiology* **474**, 291–301.

WILLIAMS, D. A. & FAY, F. S. (1990). Intracellular calibration of the fluorescent calcium indicator Fura-2. *Cell Calcium* **11**, 75–83.

YUE, D. T., MARBAN, E. & WEIR, W. G. (1986). Relationship between force and intracellular $[Ca^{2+}]$ in tetanized mammalian heart muscle. *Journal of General Physiology* **87**, 223–242.

ZAHALAK, G. I. & MA, S. P. (1990). Muscle activation and contraction: constitutive relations based directly on cross-bridge kinetics. *Journal of Biomechanical Engineering* **112**, 52–62.

Acknowledgements

This work was supported by National Institutes of Health grant HL35032 (F.J.J) and an OSP grant from Monash University (D.L.M.).

Author's email address

D. R. Claflin: claflin@zeus.bwh.harvard.edu

Received 19 December 1995; accepted 3 December 1996.